Journal of Information Hiding and Multimedia Signal Processing ©2017 ISSN 2073-4212
Ubiquitous International Volume **8**, Number **2**, March **2017**

Multi-Bit Reversible Data Hiding with Prediction and Difference Alteration

Hsiang-Cheh Huang

Department of Electrical Engineering
National University of Kaohsiung
No. 700 University Road, Kaohsiung 811, Taiwan, R.O.C.
hch.nuk@gmail.com

Feng-Cheng Chang *

Department of Innovative Information and Technology
Tamkang University
No. 180 Linwei Road, Jiaosi, Ilan 262, Taiwan, R.O.C.
* : Corresponding author.
135170@mail.tku.edu.tw

Yuh-Yih Lu

Department of Electrical Engineering
Minghsin University of Science and Technology
No.1, Xinxing Rd., Xinfeng Hsinchu 30401, Taiwan, R.O.C.
yylu@must.edu.tw

Received September 2016; revised January 2017

Abstract. *Reversible data hiding belongs to one of the applications of digital rights management (DRM). Among the DRM applications, watermarking or data hiding techniques work along with encryption algorithms. Nowadays, people tend to capture images with smart phones, and then they can transmit the images online instantly. Therefore, DRM relating issues can be directly applicable to protect the copyright of multimedia contents, and methods with reversible data hiding have also been developed. For reversible data hiding, we can look for the marked quality of multimedia contents, the number of secret bits for embedding, and the overhead for decoding to serve as performance assessments. We employ prediction techniques to produce the predicted image, and then to calculate the differences between original image and predicted one. We embed multiple bits at a time based on the characteristics of images to look for enhanced amount of capacity. Simulation results have pointed out the enhancement in embedding capacities, and the improvements in overall performances over relating methods in literature.*

Keywords: Reversible data hiding, Prediction, Multi-bit embedding.

1. **Introduction.** Digital rights management (DRM) forms an important part in multimedia systems [1, 2]. Due to the widespread use of smart phones or tablets, and the availability of easily accessed wireless networks, people tend to view the multimedia contents with browsers, or capture images and share them online with social networking service instantly. Based on the observation that the vast amount of multimedia files transmitted over the Internet, DRM issues such as copyright protection have attracted

more and more attention, and reversible data hiding, working together with encryption-relating techniques [3, 4], has become an interesting topic in this field.

Reversible data hiding lies under the umbrella of watermarking. It owns the characteristics of 'reversibility' [5, 6]. It means that secret information can be hidden into original images with the algorithms devised by researchers, and the marked image can be produced at the encoder output, just like conventional steganography techniques. At the decoder, due to 'reversibility', embedded secret and original image should be perfectly separated from marked image, with the possible provision of side information. Thus, how to keep the reversibility of devised algorithm would be the major concern for research [7, 8].

Besides the requirement of reversibility, there are other performance metrics to assess the effectiveness of algorithms in reversible data hiding. Marked image quality would be the major concern for the design of algorithms because the marked image should look alike the original one subjectively. Regarding to the objective measures of image quality, the peak signal-to-noise ratio (PSNR) is commonly employed. Larger PSNR values imply better quality of marked images [9, 10]. In addition, the size of secret information, or the number bits for embedding, also called the capacity, should also be observed. For embedding the larger amount of capacity, more alteration to the original image can be expected, and hence the more degradation to the marked image quality might be resulted [11, 12]. In this paper, we aim at devising algorithms for the enhanced capacity with acceptable quality of marked images. Furthermore, the possible overflow in the marked image after secret embedding may also be encountered. To keep the reversibility, side information, such as the location map (LM), may need to be recorded to avoid possible overflow occurred [13, 14]. Hence, the tradeoff among the marked image quality, the capacity, and the side information should be considered for the design of reversible data hiding algorithms.

In this paper, we aim at the enhancements of embedding capacities for prediction-based reversible data hiding. Unlike embedding one bit at a time, we propose to embed multiple bits at a time with the alteration of difference values between the predicted image and the original one. Relationships between embedding capacity and marked image quality can be compared with the simulation results provided.

This paper is organized as follows. In Sec. 2, we briefly describe two methods with the use of prediction-based difference alteration for reversible data hiding. In Sec. 3, we propose to embed multi-bit at a time to look for enhanced capacity. We also perform comparisons to relating papers with multi-bit embedding in literature. Experimental results are demonstrated in Sec. 4, and enhancements in capacity can be observed. Proposed methods perform generally better than conventional ones in literature. Finally, we give the conclusion of this paper in Sec. 5.

2. **Conventional Schemes.**

Conventional schemes in reversible data hiding can be classified into two categories by considering the inherent characteristics of original images. The first one is by modifying the difference value between neighboring pixels [15, 16] based on the local characteristics of original images. And the other is by altering the histogram of original image [17, 18] by considering the global characteristics. Both of them have their advantages and drawbacks. For the former category, large amounts of bits can be expected for hiding. On the other hand, for the latter category, it is famous for guaranteed quality of marked image with low overhead produced.

For the assessment of reversible data hiding algorithms, the reversibility should be guaranteed. Next, the marked image quality can be measured with the peak signal-to-noise ratio (PSNR) with the unit of decibel (dB). Larger PSNR value implies better image quality. Thirdly, the amount of secret bits for hiding, called capacity, can be expected

as large as possible. For fair comparisons, we can use the ratio between the number of secret bits and the size of original image, with the unit of bit per pixel (bpp), to present the capacity. Finally, for guaranteed reversibility of algorithm, some side information or overhead should be required. The side information should be as few as possible.

We may tend to develop the reversible data hiding algorithm with the advantages from both the categories, including large number of bits for hiding, guaranteed quality, and small amounts of overhead. Therefore, by use of some kind of difference values with the histogram alteration method seems an applicable approach. Because the marked image is expected to look like its original counterpart, we may produce a predicted image to help hiding the secret bits. With the proper alteration of the difference histogram between original and predicted images, large amounts of secret bits can be embedded, and then the marked image can be produced.

There are lots of prediction schemes in literature. Considering the ease of implementation, we choose two schemes [19, 20] for performing reversible data hiding. They are briefly described as follows.

Method 1. In Method 1, we employ the concept from [19]. Suppose the original image I has the size of $M \times N$. The first row and the first column of original image $I(x, y)$ are reserved as reference pixels. Predicted image can be calculated with

$$\hat{I}(x, y) = \left\lfloor \frac{1}{2} \left(I(x-1, y) + I(x, y-1) \right) \right\rfloor. \tag{1}$$

Next, the difference between the two can be calculated by

$$d = \left| I(x, y) - \hat{I}(x, y) \right|. \tag{2}$$

With the chosen threshold T for embedding the secret bit b, pixel values in the marked image $I'(x, y)$ can be derived from one of the two cases below.

- If $d \leq T$, the secret bit b can be embedded, and then $I'(x, y)$ can be calculated by

$$I'(x, y) = \begin{cases} \hat{I}(x, y) + 2d + b, & \text{if } \hat{I}(x, y) < I(x, y); \\ \hat{I}(x, y) - 2d - b, & \text{otherwise.} \end{cases} \tag{3}$$

- If $d > T$, the secret bit cannot be embedded, and then $I'(x, y)$ can be represented by

$$I'(x, y) = \begin{cases} \hat{I}(x, y) + T + 1, & \text{if } \hat{I}(x, y) < I(x, y); \\ \hat{I}(x, y) - T - 1, & \text{otherwise.} \end{cases} \tag{4}$$

For the original image with the size of $M \times N$, because the first row and the first column are kept unchanged to serve as the reference, only $(M-1) \times (N-1)$ pixels may be suitable for data embedding, leading to the maximal capacity of $\frac{(M-1)\times(N-1)}{M\times N}$ bpp. Hence, the maximal capacity would be expected to be less than 1 bpp with the method in [19].

Method 2. In Method 2, we choose the idea from [20]. The concept of image subsampling can be employed [17]. We use one simple example with the original image size of 4×4 to describe the image prediction scheme. In Fig. 1, each small square represents one pixel.

In Fig. 1(a), pixels in green, denoted by R_1 to R_4, represent the reference pixels. Remaining pixels in white, denoted by E_1 to E_{12}, represent the embeddable pixels. In Fig. 1(b), with the reference pixels, and by use of bilinear interpolation, the interpolated pixels I_1 to I_{12} shown in red and yellow, which correspond to the pixel positions in white, can be obtained. Next, difference values, d, can be obtained with the subtraction between Fig. 1(a) and Fig. 1(b), and then the difference histogram can be acquired. With the

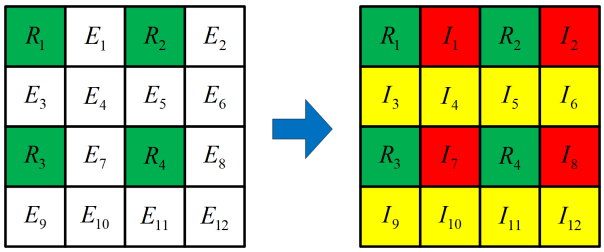

(a) (b)

FIGURE 1. (a) The 4×4 original image. Pixels in green are reference pixels, and remaining pixels are embeddable pixels. (b) The predicted image. Pixels in yellow are predicted from their counterparts in Fig. 1(a).

pre-determined threshold T for embedding the secret bit b, embeddable pixels can be modified with the following.

- If $|d| \leq T$, the embeddable pixels after modification can be represented by

$$E'_l = I_l + 2d + b. \tag{5}$$

- If $|d| > T$,

$$E'_l = \begin{cases} E_l + (T+1), & \text{if } d \geq 0; \\ E_l - (T+1), & \text{otherwise.} \end{cases} \tag{6}$$

Next, in order to look for the increased embedding capacity, we can also check whether the reference pixels can be embeddable or not. By following Eqs. (5) and (6):

- If $|d| \leq T$, the embeddable pixels after modification can be represented by

$$R'_l = E'_l + 2d + b. \tag{7}$$

- If $|d| > T$,

$$R'_l = \begin{cases} R_l + (T+1), & \text{if } d \geq 0; \\ R_l - (T+1), & \text{otherwise.} \end{cases} \tag{8}$$

Again, corresponding to Method 1 in [19], the maximal capacity would be expected to be less than 1 bpp with Method 2 in [20].

3. **Multi-Bit Reversible Data Embedding.** We can easily observe that the embedding capacities for both Method 1 [19] and Method 2 [20] are less than 1.0 bpp. By use of the alteration of histogram, if we can embed multiple bits at a time, enhancements in embedding capacity can be observed. However, degraded quality of marked image due to the more alterations to the original image can also be expected. For decoding, secret bits and original image should be perfectly separated from marked image. With the provision of side information, multiple bits at a time can be extracted from multiple values of the difference histogram. Original image can also be recovered correspondingly. Thus, we may look for the performances with larger capacity and acceptable quality for reversible data hiding.

For multi-bit embedding, we take two-bit bedding for instance. We plan to embed b_1b_2 into original image. For the difference histogram at positive portion, the bits values can fit one of the four cases below:

- For $b_1b_2 =$ '00', we add the original value by 0, or keep the original value unchanged.
- For $b_1b_2 =$ '01', we add the original value by 1.
- For $b_1b_2 =$ '10', we add the original value by 2.

- For $b_1b_2 =$ '11', we add the original value by 3.

For the difference histogram at negative portion, the same manner can be applied by subtracting the designated values.

Corresponding to Method 1 in [19], for embedding two bits b_1b_2 at a time, Eq. (3) can be changed to

$$I'(x,y) = \begin{cases} \hat{I}(x,y) + 2d + b_1b_2, & \text{if } \hat{I}(x,y) < I(x,y); \\ \hat{I}(x,y) - 2d - b_1b_2, & \text{otherwise.} \end{cases} \tag{9}$$

Accordingly, for embedding two bits at a time in Method 2 in [20], the embeddable pixels and reference pixels can be transformed to

$$E'_l = I_l + 2 \cdot d + b_1b_2, \text{ and} \tag{10a}$$

$$R'_l = E'_l + 2 \cdot d + b_1b_2. \tag{10b}$$

For larger difference values between original and predicted images at some pixel location (i,j), after embedding, if the new difference value lies outside the range of $[-255, 255]$, such a location is designated to be unsuitable for data hiding. For keeping the reversibility, by following the concepts in [23], such a location (i,j) should be recorded into the location map, with the length of $\lceil \log_2 M \rceil + \lceil \log_2 N \rceil$-bit.

We also look for similar methods for multiple bits embedding in [21] and [22] for comparisons. With multi-bit embedding for Method 1 and Method 2, they are famous for the low overhead required. For [21] and [22], in order to look for enhanced capacity, increased number of overhead may be observed, which leads to the major drawback of relating methods.

4. **Experimental Results.** We have conducted experiments with eight images in total, including `airplane`, `boat`, `couple`, `F16`, `Lena`, `pepper`, `truck`, and `Zelda`. All the images have the sizes of 512×512.

In Table 1, we present the maximally allowable embedding capacity with the four methods in [19], [20], [21], and [22] in literature. When we observe the capacity along, except for the couple image, we can find that the multi-bit embedding with Method 1 reach the largest capacity among the four methods in all the other seven images. Because larger embedding capacity would lead to degraded quality of output image, it would be necessary to look for different embedding capacity with corresponding output quality for comparisons among the methods.

In Fig. 2, we present the performances with the `airplane` image. Fig. 2(a) shows the marked image after embedding the maximal capacity of 1.9346 bpp, which leads to the image quality of 27.50 dB. Fig. 2(b) depicts the performance comparisons among the four methods. Multi-bit embedding for Method 1 has the largest capacity, and performs well in general. Huang's method in [21] performs a bit better than Method 1, however, it suffers from the increased overhead for decoding due to the algorithm design. The maximally allowable capacities with the four methods all surpass 1.0 bpp.

In Fig. 3, we display the performances with the `boat` image. Fig. 3(a) illustrates the marked image after embedding the maximal capacity of 1.4346 bpp, which leads to the image quality of 22.19 dB. Fig. 3(b) depicts the performance comparisons among the four methods. Again, the maximally allowable capacities with the four methods all surpass 1.0 bpp. Even though the multi-bit embedding for Method 1 leads to the largest capacity, Huang's method in [21] performs generally better than the others.

In Fig. 4, we present the performances with the `couple` image. Fig. 4(a) shows the marked image after embedding the maximal capacity of 1.3657 bpp, which leads to the image quality of 23.76 dB. Fig. 4(b) depicts the performance comparisons among the four

TABLE 1. Comparisons of maximally allowable capacity with corresponding image quality for the eight test images.

Method / Image	Method 1	Method 2	In [21]	In [22]
airplane	1.9346 bpp 27.50 dB	1.8846 bpp 24.05 dB	1.7404 bpp 31.07 dB	1.4746 bpp 26.28 dB
boat	1.4346 bpp 22.19 dB	1.1266 bpp 22.31 dB	1.0660 bpp 27.98 dB	1.3705 bpp 20.95 dB
couple	1.3657 bpp 23.76 dB	1.0852 bpp 22.66 dB	1.0653 bpp 30.93 dB	1.3748 bpp 21.95 dB
F16	1.8291 bpp 24.87 dB	1.7588 bpp 23.13 dB	1.4821 bpp 29.07 dB	1.4134 bpp 23.66 dB
Lena	1.8738 bpp 23.66 dB	1.7608 bpp 21.76 dB	1.5435 bpp 28.87 dB	1.4395 bpp 22.94 dB
pepper	1.7396 bpp 23.36 dB	1.4439 bpp 23.32 dB	1.3099 bpp 28.80 dB	1.4384 bpp 22.65 dB
truck	1.7435 bpp 22.84 dB	1.5678 bpp 21.17 dB	1.1125 bpp 29.51 dB	1.4351 bpp 21.50 dB
Zelda	1.9697 bpp 24.75 dB	1.7022 bpp 22.24 dB	1.6322 bpp 29.17 dB	1.4738 bpp 23.57 dB

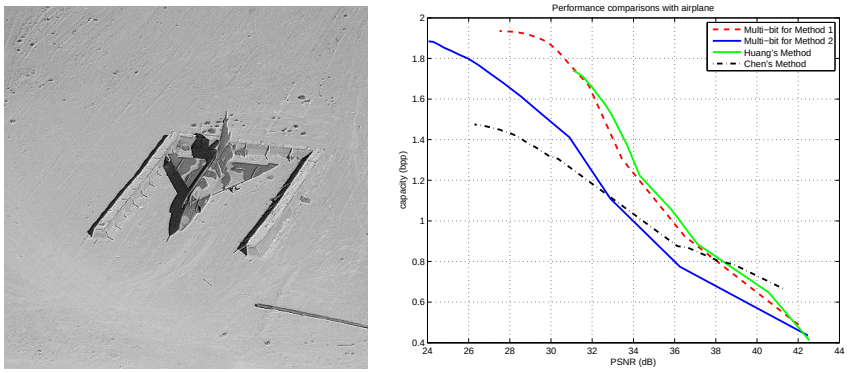

(a) (b)

FIGURE 2. (a) Subjective comparison for airplane with maximal capacity of 1.9346 bpp, PSNR = 27.50 dB. (b) Performances with relating methods.

methods. We first find that the maximally allowable capacities with the four methods all surpass 1.0 bpp. Even though the multi-bit embedding for Method 1 performs better at larger capacity regions, Huang's method in [21] and Chen's method in [22] outperform the others due to the complicated design of algorithms.

In Fig. 5, we depict the performances with the F16 image. Fig. 5(a) presents the marked image after embedding the maximal capacity of 1.8291 bpp, which leads to the image quality of 24.87 dB. Fig. 5(b) shows the performance comparisons among the four methods. The maximally allowable capacities with the four methods all surpass 1.0 bpp. Method 1 performs better at larger capacity region, and Huang's method in [21] outperforms Method 1 by a slight margin in other capacity region. Both Method 1 and Huang's method in [21] outperform other methods.

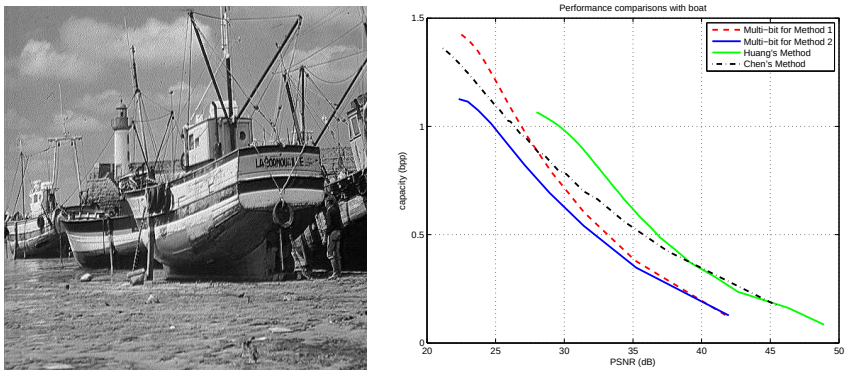

(a) (b)

FIGURE 3. (a) Subjective comparison for `boat` with maximal capacity of 1.4346 bpp, PSNR = 22.19 dB. (b) Performances with relating methods.

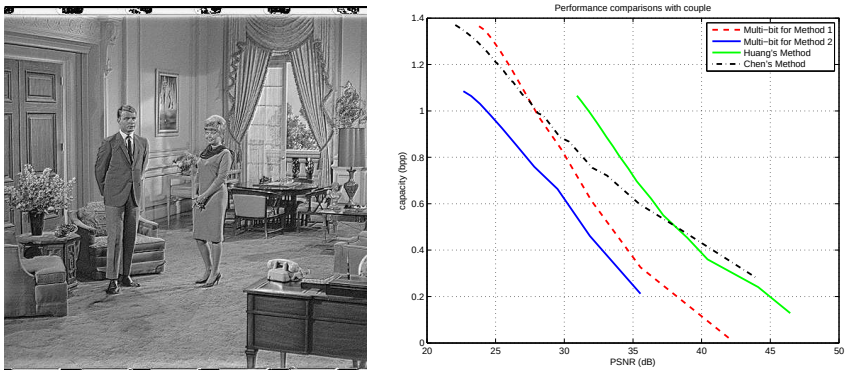

(a) (b)

FIGURE 4. (a) Subjective comparison for `couple` with maximal capacity of 1.3657 bpp, PSNR = 23.76 dB. (b) Performances with relating methods.

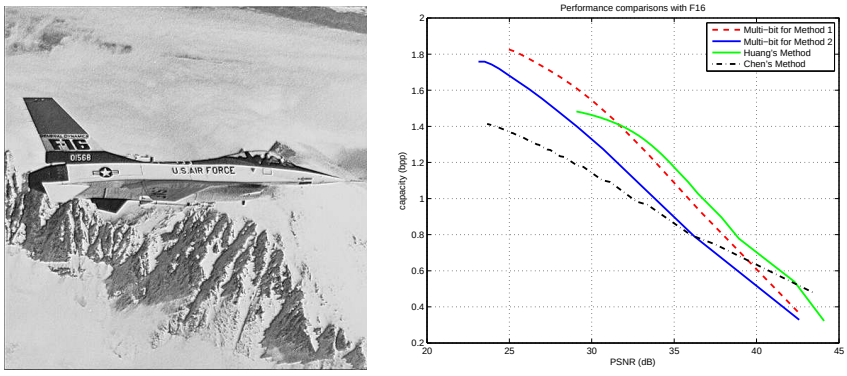

(a) (b)

FIGURE 5. (a) Subjective comparison for `F16` with maximal capacity of 1.8291 bpp, PSNR = 24.87 dB. (b) Performances with relating methods.

In Fig. 6, we show the performances with the `Lena` image. Fig. 6(a) presents the marked image after embedding the maximal capacity of 1.8738 bpp, which leads to the image quality of 23.66 dB. Fig. 6(b) presents the performance comparisons among the

four methods. Huang's Method in [21] works well in most cases, however, the maximally allowable capacities with Method 1 and Method 2 outperform the other two methods.

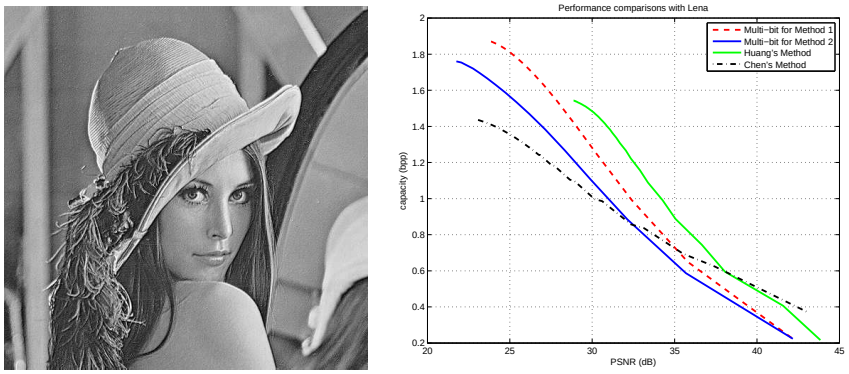

(a) (b)

FIGURE 6. (a) Subjective comparison for `Lena` with maximal capacity of 1.8738 bpp, PSNR = 23.66 dB. (b) Performances with relating methods.

In Fig. 7, we display the performances with the pepper image. Fig. 7(a) illustrates the marked image after embedding the maximal capacity of 1.7396 bpp, which leads to the image quality of 23.36 dB. Fig. 7(b) depicts the performance comparisons among the four methods. Even though Huang's method in [21] performs well in most cases, it reaches the smallest value of allowable embedding capacity among the four methods. Method 1 works well because the capacity surpasses its counterpart in Huang's method by 32.8%.

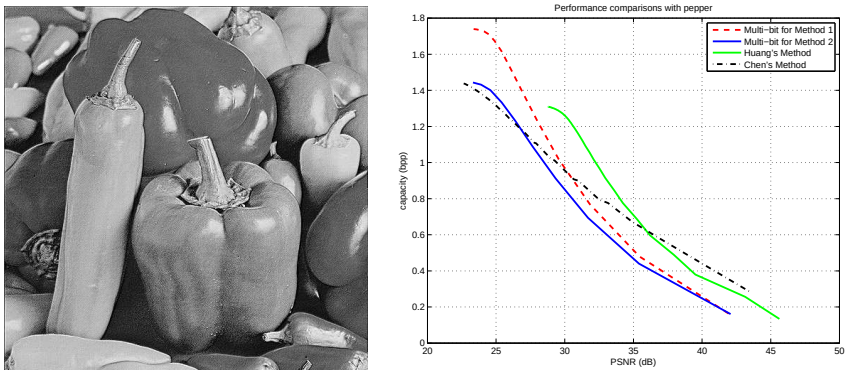

(a) (b)

FIGURE 7. (a) Subjective comparison for `pepper` with maximal capacity of 1.7396 bpp, PSNR = 23.36 dB. (b) Performances with relating methods.

In Fig. 8, we present the performances with the `truck` image. Fig. 8(a) shows the marked image after embedding the maximal capacity of 1.7435 bpp, which leads to the image quality of 22.84 dB. Fig. 8(b) displays the performance comparisons among the four methods. Huang's method in [21] performs generally good under its allowable capacity. However, capacities with the other three methods outperform that in Huang's method by a large margin, with the increase from 29.00% to 56.72%. Here, Method 1 performs better than Method 2 and Chen's method in [22].

Finally, in Fig. 9, we depict the performances with the `Zelda` image. Fig. 9(a) presents the marked image after embedding the maximal capacity of 1.9697 bpp, which leads to the image quality of 24.75 dB. Fig. 9(b) shows the performance comparisons among the

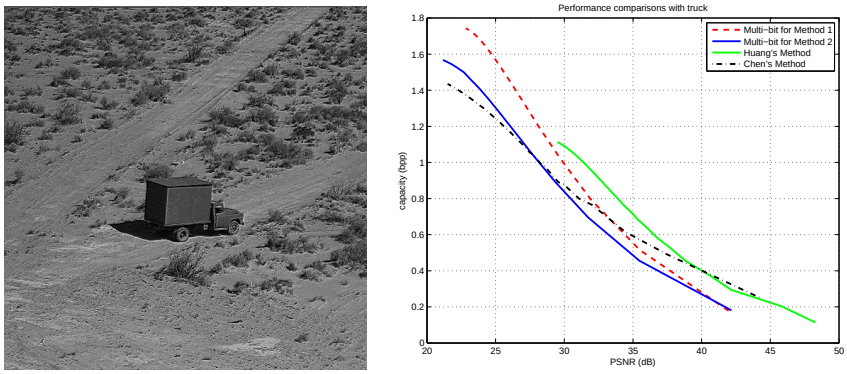

(a) (b)

FIGURE 8. (a) Subjective comparison for `truck` with maximal capacity of 1.7435 bpp, PSNR = 22.84 dB. (b) Performances with relating methods.

four methods. Again, Huang's method in [21] has its limitation in maximal allowable capacity. Method 1 performs better than Huang's method by 20.68%. Huang's method performs well under its allowable capacity. For larger capacities, Method 1 can replace Huang's method with acceptable image quality.

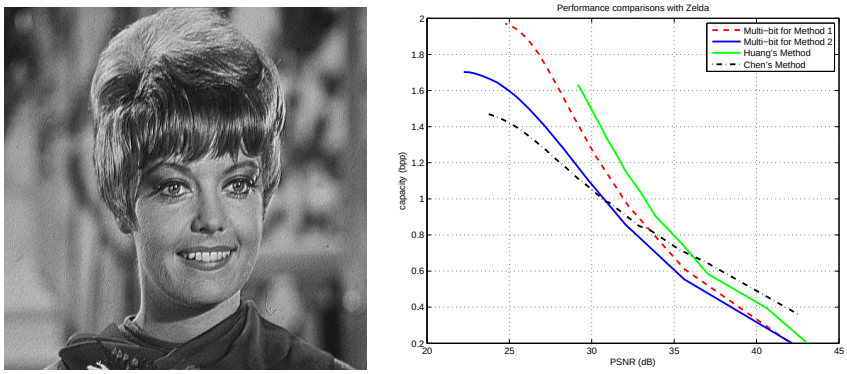

(a) (b)

FIGURE 9. (a) Subjective comparison for `Zelda` with maximal capacity of 1.9697 bpp, PSNR = 24.75 dB. (b) Performances with relating methods.

Summing up, Method 1 and Method 2 are famous for their ease of implementation. Between them, Method 1 performs better. Considering relating methods in [21] and [22], reversible data hiding can be achieved with the block-based matter. It would lead to the overhead for correctly decoding at the receiver. With the simulations in the eight images, Huang's method performs well; however, it has inferior performances in embedding capacity to compare to other methods. For large embedding capacities, Method 1 indicates good performances, and it has the attraction of easy implementation and small overhead needed.

5. **Conclusions.** In this paper, we have presented the reversible data hiding algorithms with prediction-based difference alteration method. To generate the difference values for reversible data hiding, we apply similar schemes in prediction and subsampling, and alter the difference histogram for hiding secret information. Better performances with larger capacities can be observed from the simulations. Therefore, in order to look for the

balance among quality, capacity, and side information, multi-bit embedding for Method 1 would be a good choice. We may borrow the concepts from relating methods to adaptively embed single- or multi-bit at a time, and look for the opportunity to reach the tradeoff among the guaranteed reversibility, the better image quality, and the larger embedding capacity.

Acknowledgment. This is supported in part by Ministry of Science and Technology (Taiwan, R.O.C.) under grants MOST104-2221-E-390-012 and MOST105-2221-E-390-022.

REFERENCES

[1] Y.H. Chen and H.C. Huang, "Coevolutionary genetic watermarking for owner identification, *Neural Computing and Applications*, vol. 26, no. 2, pp. 291–298, Feb. 2015.
[2] H.C. Huang and W.C. Fang, Metadata-based image watermarking for copyright protection, *Simulation Modelling Practice and Theory*, vol. 18, no. 4, pp. 436–445, Apr. 2010.
[3] H.C. Huang, Y.Y. Lu, and J. Lin, Ownership protection for progressive image transmission with reversible data hiding and visual secret sharing, *Optik*, vol. 127, no. 15, pp. 5950–5960, Aug. 2016.
[4] F.C. Chang, H.C. Huang, and H.M. Hang, Combined encryption and watermarking approaches for scalable multimedia coding, *Lecture Notes in Computer Science*, vol. 3333, pp. 356–363, 2004.
[5] Y.Q. Shi, X. Li, X. Zhang, H.T. Wu, and B. Ma, Reversible data hiding: Advances in the past two decades, *IEEE Access*, vol. 4, pp. 3210–3237, May 2016.
[6] X. Hu, *et al.*, Minimum rate prediction and optimized histograms modification for reversible data hiding, *IEEE Trans. Infor. Forensics & Security*, vol. 10, no. 3, pp. 653–664, Mar. 2015.
[7] Z. Ni, Y.Q. Shi, N. Ansari, and W. Su, Reversible data hiding, *IEEE Trans. Circuits Syst, Video Technol.*, vol. 16, no. 3, pp. 354–362, Mar. 2006.
[8] H.J. Kim, *et al.*, A novel difference expansion transform for reversible data embedding, *IEEE Trans. Infor. Forensics & Security*, vol. 3, no. 3, pp. 456–465, Sep. 2008.
[9] X. Li, *et al.*, A novel reversible data hiding scheme based on two-dimensional difference-histogram modification, *IEEE Trans. Infor. Forensics & Security*, vol. 8, no. 7, pp. 1091–1100, Jul. 2013.
[10] H.C. Huang and W.C. Fang, Techniques and applications of intelligent multimedia data hiding, *Telecommunication Systems*, vol. 44, no. 3-4, pp. 241–251, Aug. 2010.
[11] H.C. Huang and F.C. Chang, Multi-tier and multi-bit reversible data hiding with contents characteristics, *J. Information Hiding and Multimedia Signal Proc.*, vol. 7, no. 1, pp. 11–20, Jan. 2016.
[12] H.C. Huang, F.C. Chang, W.C. Fang, and S.H. Li, Reversible data hiding with prediction-based histogram alteration, *Research Notes in Information Sciences*, vol. 13, pp. 84–87, 2013.
[13] W. Zhang, H. Wang, D. Hou, and N. Yu, Reversible data hiding in encrypted images by reversible image transformation, *IEEE Trans. Multimedia*, vol. 18, no. 8, pp. 1469–1479, Aug. 2016.
[14] I.F. Jafar, K.A. Darabkh, R.T. Al-Zubi, and R.R. Saifan, An efficient reversible data hiding algorithm using two steganographic images, *Signal Processing*, vol. 128, pp. 98–109, Nov. 2016.
[15] X. Li, B. Li, B. Yang, and T. Zeng, General framework to histogram-shifting-based reversible data hiding, *IEEE Trans. Image Processing*, vol. 22, no. 6, pp. 2181–2191, Jun. 2013.
[16] A.M. Alattar, Reversible watermark using the difference expansion of a generalized integer transform, *IEEE Trans. Image Processing*, vol. 13, no. 8, pp. 1147–1156, Aug. 2004.
[17] H.C. Huang and F.C. Chang, Hierarchy-based reversible data hiding, *Expert Systems with Applications*, vol. 40, no. 1, pp. 34–43, Jan. 2013.
[18] Y.H. Chen, H.C. Huang, and C. Lin, Block-based reversible data hiding with multi-round estimation and difference alteration, *Multimedia Tools & Appli.*, vol. 75, no. 21, pp. 13679–13704, Nov. 2016.
[19] C.F. Lee, H.L. Chen, and H.K. Tso, Embedding capacity raising in reversible data hiding based on prediction of different expansion, *J. Syst. and Software*, vol. 83, no. 10, pp. 1864–1872, Oct. 2010.
[20] T.C. Lu, *et al.*, High capacity reversible hiding scheme based on interpolation, difference expansion, and histogram shifting, *Multimedia Tools & Appli.*, vol. 72, no. 1, pp. 417–435, Sep. 2014.
[21] H.C. Huang, Y.H. Chen, F.C. Chang and S.H. Li, Multi-level reversible data hiding with prediction-based approach, *Information*, vol. 16, no. 8(B), pp. 6069–6078, Aug. 2013.
[22] C.C. Chen and Y.H. Tsai, Adaptive reversible image watermarking scheme, *J. Syst. and Software*, vol. 84, no. 3, pp. 428–434, Mar. 2011.
[23] F.C. Chang and H.C. Huang, Reversible data hiding with difference prediction and content characteristics, *J. Infor. Hiding and Multimedia Signal Proc.*, vol. 7, no. 3, pp. 599–609, May 2016.